*Protein Science* (1999), *8*:1241–1249. Cambridge University Press. Printed in the USA.


# Oligomeric integrity—The structural key to thermal stability in bacterial alcohol dehydrogenases

YAKOV KORKHIN,[1,4] A. JOSEPH KALB(GILBOA),[1] MOSHE PERETZ,[2] OREN BOGIN,[2] YIGAL BURSTEIN,[2] AND FELIX FROLOW[3,5]

[1]Department of Structural Biology, The Weizmann Institute of Science, Rehovot 76100, Israel
[2]Department of Organic Chemistry, The Weizmann Institute of Science, Rehovot 76100, Israel
[3]Department of Chemical Services, The Weizmann Institute of Science, Rehovot 76100, Israel

(RECEIVED December 31, 1998; ACCEPTED March 18, 1999)

**Abstract**

Principles of protein thermostability have been studied by comparing structures of thermostable proteins with mesophilic counterparts that have a high degree of sequence identity. Two tetrameric NADP(H)-dependent alcohol dehydrogenases, one from *Clostridium beijerinckii* (CBADH) and the other from *Thermoanaerobacter brockii* (TBADH), having exceptionally high (75%) sequence identity, differ by 30° in their melting temperatures. The crystal structures of CBADH and TBADH in their holo-enzyme form have been determined at a resolution of 2.05 and 2.5 Å, respectively. Comparison of these two very similar structures (RMS difference in C$\alpha$ = 0.8 Å) revealed several features that can account for the higher thermal stability of TBADH. These include additional ion pairs, "charged-neutral" hydrogen bonds, and prolines as well as improved stability of $\alpha$-helices and tighter molecular packing. However, a deeper structural insight, based on the location of stabilizing elements, suggests that enhanced thermal stability of TBADH is due mainly to the strategic placement of structural determinants at positions that strengthen the interface between its subunits. This is also supported by mutational analysis of structural elements at critical locations. Thus, it is the reinforcement of the quaternary structure that is most likely to be a primary factor in preserving enzymatic activity of this oligomeric bacterial ADH at elevated temperatures.

**Keywords:** alcohol dehydrogenase; crystal structure; oligomers; mutagenesis; thermal stability

What enables a protein to withstand elevated temperatures or harsh chemical conditions without losing its biological activity is a question of theoretical and practical importance. To address this question, crystal structures of several thermostable proteins, both monomeric and oligomeric, have been determined and compared to those of their mesophilic counterparts (Jaenicke, 1996). These studies point to a number of stabilizing interactions as structural determinants of thermostability. These include stabilization of the structure and dipole moments of $\alpha$-helices (Hol et al., 1978; Argos et al., 1979; Nicholson et al., 1988; Davies et al., 1993; Russell et al., 1994), increased number of proline residues in $\beta$-turns and external loops (Matthews et al., 1987; Watanabe et al., 1991), salt bridges (Perutz & Raidt, 1975; Perutz, 1978; Walker et al., 1980; Hennig et al., 1995), increase in the number of interactions between charged side chains and neutral partners ("charged-neutral" hydrogen bonds) (Tanner et al., 1996), and improvement of hydrophobic interactions and oligomeric rearrangements that fill existing cavities and lead to tighter molecular packing (Kirino et al., 1994; Delboni et al., 1995; Salminen et al., 1996). Salt-bridge networks, energetically more favorable than isolated ion pairs (Horovitz et al., 1990), have been suggested as the most prominent structural feature responsible for the unusual properties of hyperthermophiles (Hennig et al., 1995; Korndorfer et al., 1995; Yip et al., 1995; Tanner et al., 1996; Wallon et al., 1997). It has been noted that there is usually no single factor that makes a protein withstand elevated temperatures. Rather, this is accomplished through a complex combination of subtle changes specific to each protein (Matthews et al., 1974). In certain cases, effects of the above structural determinants on thermal stability have been tested by site-directed mutagenesis (Matthews et al., 1987; Hurley et al., 1992; Tomschy et al., 1994; Watanabe et al., 1994; Moriyama et al., 1995; Van den Burg et al., 1998; Vetriani et al., 1998), but no generalization that explains the underlying principles of stabilization has emerged from these studies (for a recent review see Jaenicke & Böhm, 1998).

Reprint requests to: Felix Frolow, Department of Molecular Microbiology and Biotechnology, Tel-Aviv University, Ramat Aviv 69978, Israel; e-mail: mbfrolow@ccsg.tau.ac.il.

[4]Present address: Department of Molecular Biophysics and Biochemistry, Yale University, New Haven, Connecticut 06520-8114.

[5]Present address: Department of Molecular Microbiology and Biotechnology, The George S. Wise Faculty of Life Sciences, Tel-Aviv University, Ramat Aviv 69978, Israel.

Zinc-containing NADP-dependent *sec*-alcohol dehydrogenases from *Clostridium beijerinckii* (CBADH) (Chen, 1995) and *Thermoanaerobacter* (formerly *Thermoanaerobium*) *brockii* (TBADH) (Lamed & Zeikus, 1981; Peretz & Burstein, 1989) have 75% sequence identity (Peretz et al., 1997), unusually high for proteins from different organisms, and yet they differ greatly in their thermostability temperatures of half inactivation in 60 min ($T_{1/2}^{60\ \mathrm{min}}$) are 63.8 °C for CBADH and 93.8 °C for TBADH (Bogin et al., 1998). In addition to its heat stability, TBADH also tolerates high concentrations of denaturants such as urea and organic solvents (Zeikus et al., 1979).

We have crystallized both CBADH and TBADH (Korkhin et al., 1996) and determined their structures at resolutions of 2.05 and 2.5 Å, respectively (Korkhin et al., 1998). Comparison of the three-dimensional structures shows that almost every one of the structural determinants mentioned above believed responsible for thermal stability of proteins was more frequent in TBADH. However, a deeper structural insight, taking into account the location of the additional stabilizing elements, suggests that TBADH maintains its activity at higher temperatures mainly by virtue of a fortified interface between subunits that preserves its tetrameric quaternary organization.

## Results

### *Overall comparison*

Both CBADH and TBADH are tetramers of 222 symmetry (Korkhin et al., 1996) with 351 and 352 amino acid residues per monomer, respectively, and have very similar three-dimensional structure ($\mathrm{RMSD}_{C\alpha} = 0.8$ Å). The monomer is composed of two domains separated by a deep cleft—the coenzyme binding domain with a characteristic Rossmann fold and the catalytic domain (Korkhin et al., 1998). Each monomer contains a single zinc atom in its active site, located in the catalytic domain close to the cleft between it and the cofactor-binding domain. A molecule of NADP binds to the cofactor-binding domain of each monomer, also in the area of the cleft, and is released upon reduction.

Sequence alignment of the two alcohol dehydrogenases is presented in Figure 1A. The cofactor-binding domain (residues 154–294), constituting 40% of the structure, contains 50% of all sequence differences; most of the intersubunit contacts in the tetramer are located near the cofactor-binding domain and in a protruding lobe in the catalytic domain (residues 88–109) (Fig. 1B).

### *Alpha helices*

Among the secondary structural elements that are most altered in TBADH are two interacting $\alpha$-helices of the cofactor-binding domain: $\alpha$8 (223–230) and $\alpha$9 (246–254) (Fig. 1B). These helices contain fewer polar and more hydrophobic residues in TBADH than in CBADH. In $\alpha$-helix $\alpha$9, all three serines, which have been shown to be rare in $\alpha$-helices of thermostable structures (Argos et al., 1979), are replaced by other residues, two of which are helix-favoring alanines. The dipole moment of $\alpha$8 in TBADH is stabilized (Nicholson et al., 1988; Watanabe et al., 1994) by proline P222 and glutamate E224 at its amino end. Eight of the 11 $\alpha$-helices in TBADH have at their amino ends either an acidic residue or a proline, whereas in CBADH, the N-caps of five $\alpha$-helices are stabilized.

### *Proline residues*

TBADH contains eight more proline residues (residues 22, 24, 149, 177, 222, 275, 316, and 347) than the 13 prolines present in CBADH. These are distributed more or less equally throughout the structure, but are located in structurally strategic positions. P24 is located in a $\beta$-turn at the end of an extended stretch of residues on the surface of the molecule (Watanabe et al., 1994). The flexibility of this stretch is further restrained by P22; P316 is located in an external loop of the catalytic domain between the $\alpha$-helix $\alpha$10 and the $\beta$-sheet $\beta$13; additional rigidity of this loop restrains the orientation of $\alpha$10, which is located at a subunit interface. Two prolines are located at the N-cap of $\alpha$-helices: P177 caps $\alpha$-helix $\alpha$6 and P222 caps $\alpha$8. P275 is in the center of an extended stretch of residues involved in dimerization with a second monomer, and P149 stabilizes the conformation of a sharp bend in an extended $\alpha$-helix, $\alpha$4-$\alpha$5, that interconnects the two domains of the monomer. P347 is in $\beta$-sheet $\beta$13, next to the C-terminus of the protein.

### *Ion pairs*

TBADH contains one intersubunit and two intrasubunit ion pairs in addition to the one intersubunit and nine intrasubunit ion pairs already seen in CBADH. In TBADH residue R304 from subunit A (see Fig. 1B for subunit labeling) forms an ion pair with residue E165 from subunit D and an intrasubunit ion pair with residue D237. D237 is also involved in another ion pair with residue K257. The latter ion pair is also present in CBADH; however, only in TBADH does this ion pair become part of a four-member ion pair network E165/R304/D237/K257 (Fig. 2A).

An additional intersubunit ion pair is formed in TBADH by replacements Q165E and M304R in the sequence of CBADH, and one of the intrasubunit ion pairs by replacements V224E and S254K.

The second additional intrasubunit ion pair in TBADH is formed in an unusual, indirect manner from Asp163 and Lys291, which exist in CBADH as well but are too far apart to form a salt bridge. In TBADH, however, replacement of Arg238 and Ile261 of CBADH with the smaller alanine and valine residues creates a favorable environment in the vicinity of D163 to allow its approach to residue K291 (Fig. 2B). Such an indirect mechanism for increasing the number of salt bridges in a protein by removal of an obstacle to close approach of a pair of oppositely charged groups is reported here for the first time.

### *Hydrogen bonds*

Statistics on hydrogen bonds in the structures of CBADH and TBADH are presented in Table 1. Surprisingly, there is more than a 10% decrease in the number of backbone–side-chain hydrogen bonds in TBADH vs. CBADH, but this is compensated by a 10% increase in the number of side-chain–side-chain hydrogen bonds and a 5% increase in the number of backbone–backbone hydrogen bonds, so that there is hardly any difference in the total number of hydrogen bonds between the two structures. What differences exist are mainly confined within subunits, with almost no difference in the numbers of intersubunit hydrogen bonds. In the structure of TBADH, one additional intersubunit "charged-neutral" hydrogen bond is formed between R97 of subunit A and the main-chain carbonyl oxygen of P258 of subunit B. Altogether, the structure of TBADH has 4 intersubunit and 17 intrasubunit "charged-neutral" hydrogen bonds compared to 3 intersubunit and 19 intrasubunit hydrogen bonds in the structure of CBADH.

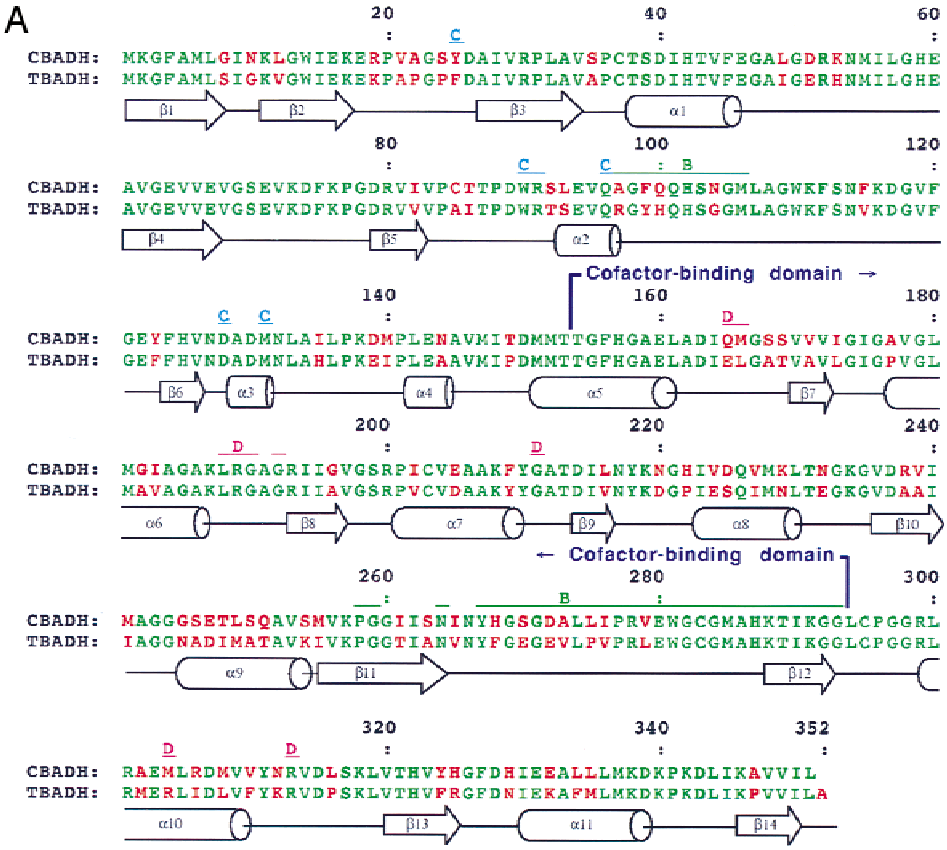


**Fig. 1. A:** Amino acid sequence alignment of alcohol dehydrogenases from CBADH and TBADH. Nonidentical residues are colored red. Residues involved in intersubunit contacts are marked above the sequences with tab marks and subunit chain id letters (relative to subunit A). Secondary structure assignment was done according to Kabsch and Sander (1983) and is marked below the sequences. **B:** Ribbon diagram of the tetramer of TBADH. The tetramer is composed of four identical subunits represented in different colors. Elements of the secondary structure in the cofactor binding domain of subunit A are marked in accordance with secondary structure assignment on Figure 1A. Generated with MOLSCRIPT (Kraulis, 1991) and RASTER3D (Merritt & Murphy, 1994).

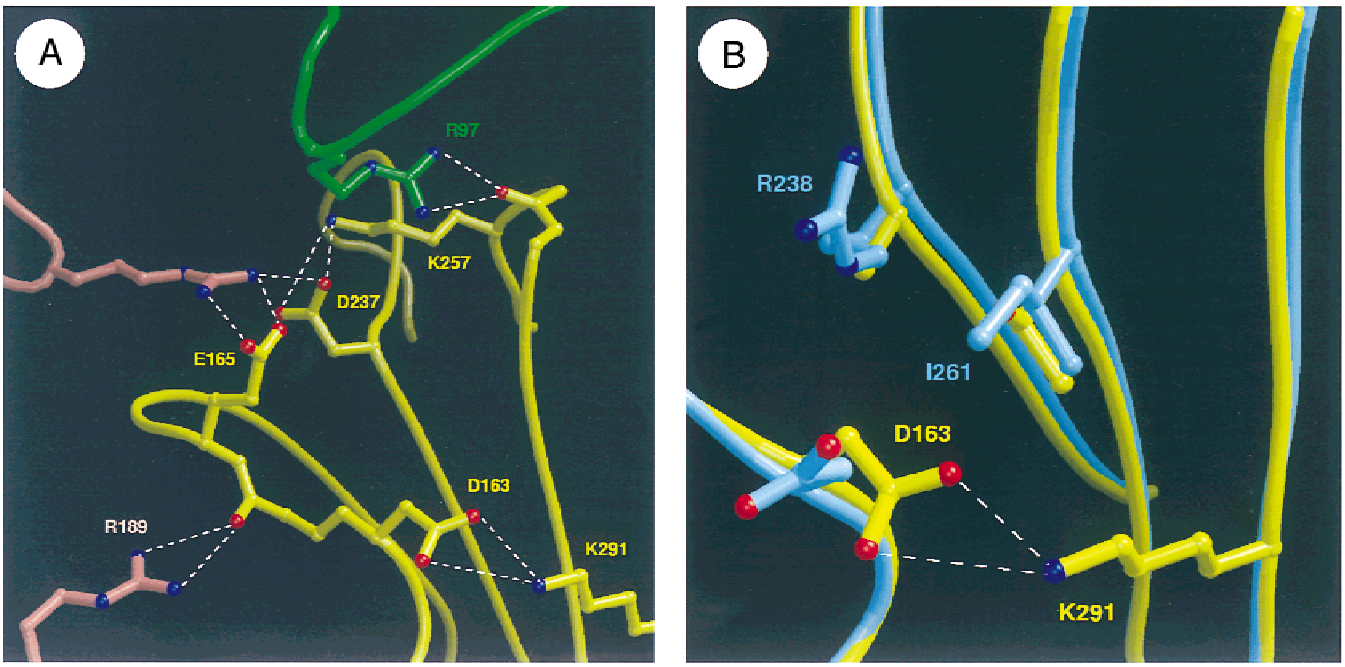


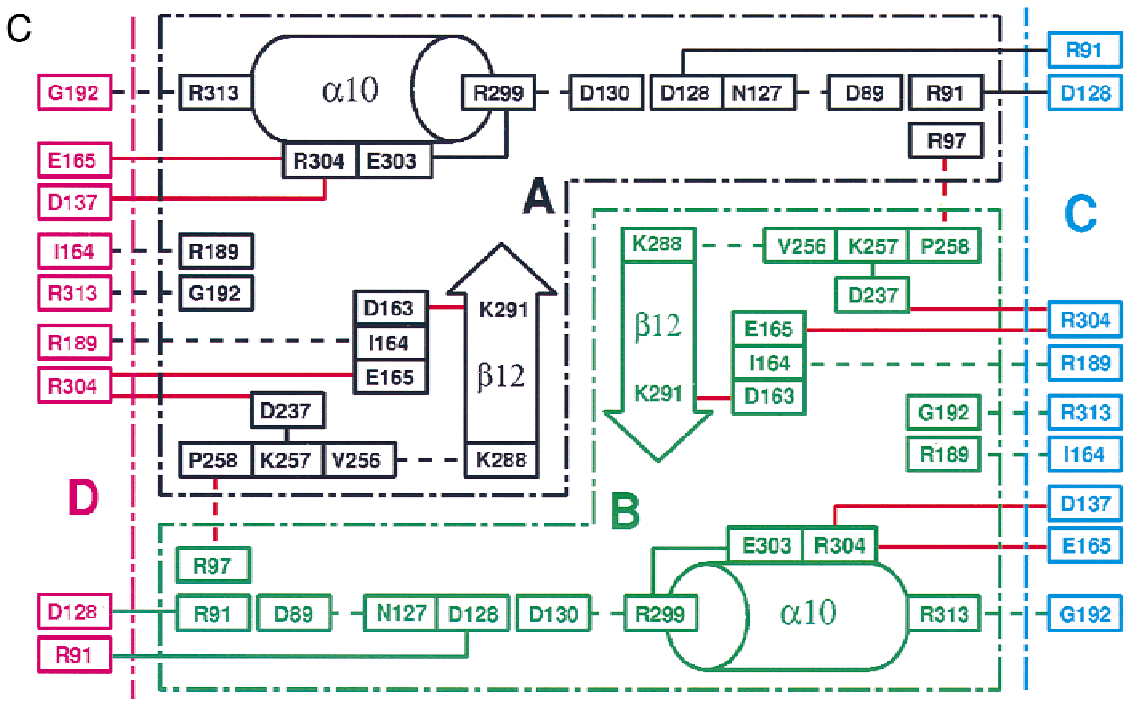


**Fig. 2.** **A:** Additional ion pairs and hydrogen bonds at the interface between subunits in TBADH. Parts belonging to different subunits are represented in their respective colors: subunit A in yellow, subunits B in green, subunit D in magenta [generated with MOLSCRIPT (Kraulis, 1991) and RASTER3D (Merritt & Murphy, 1994)]. **B:** "Indirect" way of ion pair formation in the structure of TBADH (yellow) vs. CBADH structure (light blue). Residues D163 and K291 are present in both structures, but due to replacement of R238 and I261 in CBADH by shorter alanine and valine in TBADH the local environment is favorably optimized to allow D163/K291 ion pair formation. **C:** Schematic representation of subunit interactions in TBADH. Parts belonging to different subunits are represented in their respective colors. Ion pairs are represented as solid lines; "charged-neutral" hydrogen bonds are represented as dashed lines. Interactions that are not present in CBADH are represented in red.

**Table 1.** *Hydrogen bond statistics*

| | CBADH | | | TBADH | | |
|---|---|---|---|---|---|---|
| | Intra | Inter | Total | Intra | Inter | Total |
| Backbone–backbone | 916 | 26 | 942 | 960 | 27 | 987 |
| Backbone–side chain | 348 | 53 | 401 | 304 | 56 | 360 |
| Side chain–side chain | 128 | 10 | 138 | 140 | 12 | 152 |
| | | | 1,481 | | | 1,499 |

*Molecular packing*

The total molecular accessible area of TBADH is slightly smaller (by 2.7%) than that of CBADH (Table 2). The occluded area upon tetramerization is greater by 4% for TBADH. This increase is associated with the formation of the AB, CD, AD, and BC interfaces and not the AC or BD interfaces. The number of cavities in TBADH is significantly smaller. In the case of CBADH, there are 21 intrasubunit cavities and one at the AB interface, whereas in TBADH there are six cavities, all of which are within the monomers. This improved overall packing of TBADH can contribute to its enhanced thermal stability. Specifically, there are several differences in the sequence of the two enzymes that lead to different packing in the hydrophobic core of the cofactor-binding domain (Fig. 3A). These differences are mainly in the area surrounding the $\alpha$-helix $\alpha$9, which is a supporting structural element for interacting parts of monomers A (or C) and B (or D) in the tetramer.

*Location of the stabilizing elements*

The most interesting outcome of the structural comparison between CBADH and TBADH concerns the location of the stabilizing elements with respect to quaternary organization of the enzyme. Most of the additional determinants in TBADH provide missing links or reinforce existing structural elements in the network of interactions that ensure a more stable interlock between the subunits in the tetramer of TBADH than in CBADH. The interfaces between subunits A and B and between C and D are formed by hydrophobic interactions and hydrogen bonds between $\beta$-strands $\beta$12 and stretches of residues 268–278 of both subunits. The strand $\beta$12 is part of the 12-stranded $\beta$-sheet that includes 6 $\beta$-strands from the cofactor binding domain of each of two subunits of the AB or CD dimer while the stretch 268–278 is located above it. The $\alpha$-helix $\alpha$9 provides support for the latter stretch forming a hydrophobic "cushion" between it and other parts of the cofactor-binding domain. The stretch 268–278 is extensively modified in TBADH, and the helix $\alpha$9 is the most drastically modified secondary structural element. These modifications and other modifications in the hydrophobic core of the cofactor binding domain provide a more stable interface between the two subunits (Fig. 3A). Orientation of $\alpha$9 with respect to other secondary structure elements is better secured in TBADH with an additional ion pair E224/K254 that links $\alpha$9 and $\alpha$8, which otherwise do not have substantial contact area. Substitution of H222 with a proline restrains the orientation of $\alpha$8. Substitutions in positions 273, 275, and 276 play a key role in creating better complementarity between two van der Waals surfaces at the area of interactions (Fig. 3B). Strategic introduction of a single proline residue (P275) close to the twofold axis, which relates the monomers in dimers AB and CD leads to increased rigidity of the resulting structural element and greater stability of subunit interactions in these dimers.

**Table 2.** *Molecular packing*

| | CBADH (Å$^2$) | TBADH (Å$^2$) |
|---|---|---|
| Accessible area of isolated monomers | | |
| A | 15,450 | 15,284 |
| B | 15,686 | 15,274 |
| C | 15,386 | 15,279 |
| D | 15,272 | 15,264 |
| Total | 61,794 | 61,101 |
| Total molecular accessible area of the tetramer | 47,523 | 46,254 |
| Area occluded upon tetramerization | 14,271 | 14,847 |

The role of additional ion pairs in expanding the network of subunit interactions is schematically illustrated in Figure 2C. In the structure of CBADH the mutual orientation of stretch 268–278 from subunit A (or C) and its equivalent from subunit B (or D) is stabilized at both ends of each stretch with intersubunit "charged-neutral" hydrogen bonds R278/G271. In the structure of TBADH, another "charged-neutral" hydrogen bond R97/P258 is added, which links the protruding lobe of the catalytic domain of subunit A (or C) with the cofactor-binding domain of subunit B (or D). The adjacent K257 of B (or D) makes an ion pair with D237 of the same subunit. This ion pair also exists in CBADH, but ion pairs D237/R304/E165 exist only in TBADH, thus providing an additional link to subunit C (or A) and better integration of all four subunits into the tetramer. Replacement of L316 with a proline restrains the orientation of $\alpha$10, thereby improving stability of ion pairs D237/R304/E165 and an intersubunit "charged-neutral" hydrogen bond R313/G192. The ion pair R91/D128 between subunits A and C exists in both structures, but in the structure of TBADH this intersubunit salt bridge is better protected from solvent by the hydrophobic phenylalanine residue F25, which replaces tyrosine Y25 of CBADH. The flexibility of F25, located in a $\beta$-turn, is restricted by addition of proline P24 that replaces the hydrophilic serine immediately adjacent to F25. Further, a "charged-neutral" hydrogen bond I164/R189 that links subunits C (or A) and B (or D) and is adjacent to the latter ion pair, exists also in CBADH. But an intrasubunit ion pair D163/K291, present only in TBADH, links the strand $\beta$12 to other elements of the interface between subunits and further enhances the integrity of the tetramer. Another residue, K288 of strand $\beta$12, forms a "charged-neutral" hydrogen bond with the main-chain carbonyl oxygen of V256, which is next to the ion pair network K257/D237/R304/E165. Additional reinforcement is introduced into TBADH at all subunit interfaces, increasing the strength of association between subunits throughout the entire tetramer. The general tendency is toward creating a single inseparable four-subunit entity by making the density of intersubunit interactions indistinguishable from the density of intrasubunit interactions. The particular chemical nature of structural determinants, however, is dictated by the local nature of interactions between individual subunits. Where the interface is

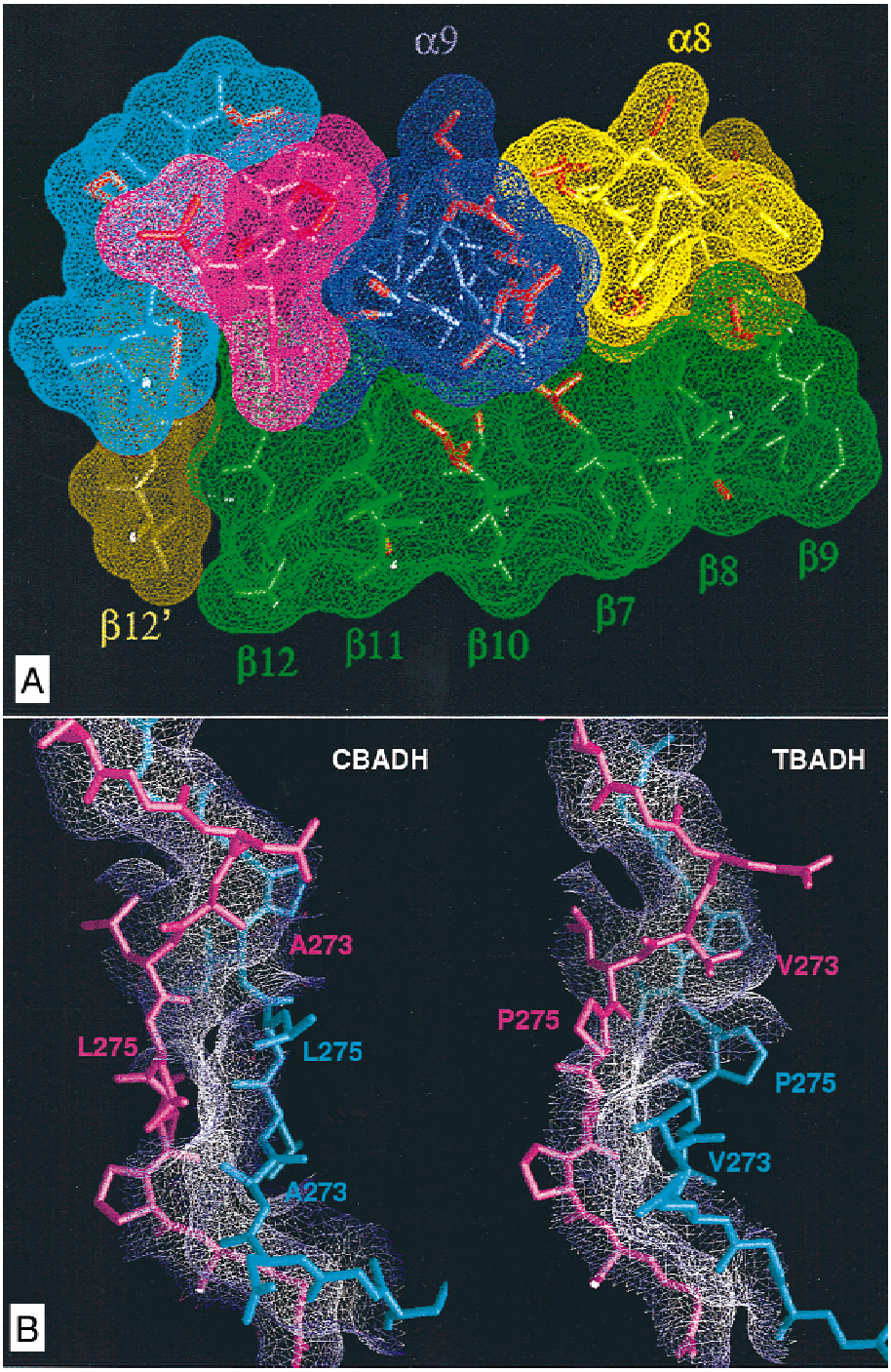


**Fig. 3. A:** Molecular surface representation of elements of secondary structure in the hydrophobic core of the cofactor binding domain of TBADH in the area of interface between subunits A and B. Secondary structure is marked in accordance with assignment presented in Figure 1A. The strand $\beta 12'$ and the stretch centered at residue P275 represented in cyan belong to subunit B; the rest of the structure belongs to subunit A. Residues that are not equivalent in CBADH and TBADH are represented in red. Helix $\alpha 9$ is the most variable region in terms of amino acid composition between the two structures. It provides hydrophobic support for the stretch of residues centered at P275 (magenta) that is involved in subunit interactions. Generated with GRASP (Nicholls et al., 1991). **B:** A view of molecular surfaces between subunits A and B. Portions of the surfaces that are further apart from each other than 2.5 Å are not shown. In the sequence of TBADH proline P275 (leucine in CBADH) is close to the noncrystallographic twofold axis leading to improved rigidity of the interacting parts of the structure. In TBADH, interacting parts have better complementarity of molecular surface and deeper interlock. Generated with GRASP (Nicholls et al., 1991).

governed by hydrophobic interactions (e.g., dimers AB and CD) additional stability is achieved by optimizing complementarity of interacting van der Waals surfaces (e.g., interactions between stretches 268–278). Where interacting parts make only a few contacts, an additional salt bridge or a "charged-neutral" hydrogen bond is added either by introducing residues that can form these interactions or by optimizing the local environment and allowing existing residues to interact (e.g., ion pair D163/K291).

## Discussion

Two general mechanisms can be proposed by which the thermostability of TBADH is increased. In the first, all the structural determinants are more or less equal participants in the effect. In this case, enhanced stability of TBADH would result from a collection of subtle changes distributed evenly throughout the structure. In the second mechanism, different structural determinants are responsible for the effect to different extents, and certain subtle changes are of greater significance than others due to their strategic location or their chemical nature. In the case of TBADH, our observations suggest the latter mechanism. Site-directed mutagenesis may shed further light on this.

Several of the above structural elements, including extra prolines (Bogin et al., 1998), salt bridges, and hydrophobic residues (Bogin et al., 1996), have been engineered by point mutation techniques into the sequence of CBADH, and the consequences for thermal stability of the enzyme were determined. Preliminary results have shown that the greatest increases in thermal stability of mutated CBADH were observed when an extra ion pair and a hydrophobic patch located at the interface between subunits were incorporated into the structure. Smaller effects were observed when intrasubunit elements of the same type were introduced (Burstein et al., 1997). This strongly suggests that TBADH retains its enzymatic activity at higher temperatures than CBADH due to a more stable interface between subunits that prevents disintegration of the tetramer; and that the greater thermal stability of TBADH is due mainly to a few strategically located structural determinants.

In 1975, Perutz suggested that in oligomeric enzymes the extra energy of stabilization can be provided "... by some extra salt bridges, hydrogen bonds or non-polar bonds at the subunit interfaces" (Perutz & Raidt, 1975). This hypothesis was supported by several subsequent studies. Comparison of the crystal structure of the tetrameric GAPDH from the thermophilic *Bacillus stearothermophilus* with that of its mesophilic counterpart from lobster muscle (Walker et al., 1980) suggested that extra thermal stability was attributable to two additional salt bridges and improved hydrophobicity of residues in an irregular S-loop that constituted a major part of the subunit interface. Increased S-loop hydrophobicity led to better contacts between subunits and to a stronger interaction in the additional intersubunit salt bridge by more effective shielding from solvent. Recently, Vetriani et al. (Vetriani et al., 1998) have observed that an intersubunit ion-pair network present in the hexameric glutamate dehydrogenase (GluDHs) from the hyperthermophile *Pyrococcus furiosus* was substantially reduced in the less stable GluDH from *Thermococcus litoralis*. They restored the missing interactions by two mutations, and improved the thermal stability of the mutant GluDH over that of the wild-type enzyme.

Nonpolar interactions at the subunit interface were shown to contribute to thermal stability of 3-isopropylmalate dehydrogenase from *Thermus thermophilus* both by X-ray crystal structure analysis (Imada et al., 1991; Moriyama et al., 1995) and by site-directed mutagenesis (Kirino et al., 1994), and of triosephosphate isomerase from *B. stearothermophilus* (Delboni et al., 1995). Thermostability was attributed to improved subunit interfaces in L-lactate dehydrogenase from *B. stearothermophilus* (Kallwass et al., 1992), malate dehydrogenase from *Thermus flavus* (Kelly et al., 1993), inorganic pyrophosphatase from *T. thermophilus* (Salminen et al., 1996), and ornithine carbamoyltransferase from *P. furiosus* (Villeret et al., 1998). Other studies also indicate that multimer formation and subunit interactions are critical for thermal stability of, for example, hemocyanin from the ancient tarantula *Eurypelma californicum* (Sterner et al., 1995), phosphoribosyl anthranilate isomerase from the hyperthermophile *Thermotoga maritima* (Hennig et al., 1997), GluDH from the hyperthermophiles *P. furiosus* (Vetriani et al., 1998), and chorismate mutase from the thermophilic archaeon *Methanococcus jannaschii* (MacBeath et al., 1998). The findings presented here also favor the correctness of Perutz's early suggestion.

## Conclusion

In summary, we have determined two three-dimensional highly homologous structures of thermostable tetrameric alcohol dehydrogenases—one from *Thermoanaerobacter brockii* (TBADH) and one from *Clostridium beijerinckii* (CBADH). TBADH and CBADH have only 25% difference in amino-acid sequence but a 26 °C difference in temperature of half inactivation. Comparison of the structures at atomic resolution reveals that TBADH has several additional structural features that can explain its increased thermal stability. These include tighter molecular packing, amino acid substitutions in two $\alpha$-helices that are known to stabilize them, additional prolines at strategically important locations, two intrasubunit ion pairs (one of which is formed by an indirect mechanism not previously observed), one ion-pair network at the subunit interface, and one intersubunit hydrogen bond between an arginyl residue and the main-chain carbonyl oxygen. However, the main reason for the greater thermal stability of TBADH is the effect of these stabilizing elements on its oligomeric integrity: the additional structural elements that are mainly responsible for thermal stabilization of TBADH are those that promote stability of the subunit interfaces in the tetramer.

Taking into account the high degree of sequence identity between the two enzymes, this structural comparison can serve as a basis for a systematic site-directed mutagenesis study aimed at quantifying the extent of thermostabilization that can be attributed to each of the above structural elements. It could also provide guidelines for engineering thermostability into other oligomeric enzymes.

## Materials and methods

Crystallization and structure determination of CBADH and TBADH have been reported earlier (Korkhin et al., 1996, 1998). Hydrogen bond networks were optimized with WHATIF (Vriend, 1990), which was also used to calculate hydrogen bond statistics and to locate ion pairs. In all calculations default geometrical parameters of the hydrogen bonds implemented in WHATIF have been used. Calculation of accessible molecular surfaces area and search for cavities were done with GRASP (Nicholls et al., 1991), using default procedures of the package. Secondary structure assignment was done according to Kabsch and Sander (1983).

## Acknowledgments

This work was supported in part by the Israel Science Foundation, founded by the Israel Academy of Sciences and the Humanities. Y.B. is the Maynard I. and Elaine Wishner Professor for Bioorganic Chemistry.

## References

Argos P, Rossmann MG, Grau UM, Suborn H, Frank G, Tratschin JD. 1979. Thermal stability and protein structure. *Biochemistry 18*:5698–5703.

Bogin O, Peretz M, Hacham Y, Korkhin Y, Frolow F, Kalb(Gilboa) AJ, Burstein Y. 1998. Enhanced thermal stability of *Clostridium beijerinckii* alcohol dehydrogenase after strategic substitution of amino acid residues with prolines from the homologous thermophilic *Thermoanaerobacter brockii* alcohol dehydrogenase. *Protein Sci 7*:1156–1163.

Bogin O, Peretz M, Korkhin Y, Frolow F, Kalb(Gilboa) AJ, Burstein Y. 1996. Thermostabilization of *Clostridium beijerinckii* alcohol dehydrogenase by site-directed mutagenesis. *Protein Sci 5*(Suppl 1):81.

Burstein Y, Bogin O, Korkhin Y, Peretz M, Kalb(Gilboa) AJ, Frolow F. 1997. Oligomeric integrity—The structural key to thermal stability in bacterial alcohol dehydrogenases. *Protein Sci 6*(Suppl 1):83.

Chen JS. 1995. Alcohol dehydrogenase: Multiplicity and relatedness in the solvent-producing clostridia. *FEMS Microbiol Rev 17*:263–273.

Davies GJ, Gamblin SJ, Littlechild JA, Watson HC. 1993. The structure of a thermally stable 3-phosphoglycerate kinase and a comparison with its mesophilic equivalent. *Proteins 15*:283–289.

Delboni LF, Mande SC, Rentierdelrue F, Mainfroid V, Turley S, Vellieux FMD, Martial JA, Hol WGJ. 1995. Crystal structure of recombinant triosephosphate isomerase from *Bacillus stearothermophilus*. An analysis of potential thermostability factors in six isomerases with known three-dimensional structures points to the importance of hydrophobic interactions. *Protein Sci 4*:2594–2604.

Hennig M, Darimont B, Sterner R, Kirschner K, Jansonius JN. 1995. 2.0-Angstrom structure of indole-3-glycerol phosphate synthase from the hyperthermophile *Sulfolobus solfataricus*—Possible determinants of protein stability. *Structure 3*:1295–1306.

Hennig M, Sterner R, Kirschner K, Jansonius JN. 1997. Crystal structure at 2.0 Å resolution of phosphoribosyl anthranilate isomerase from the hyperthermophile *Thermotoga maritima*: Possible determinants of protein stability. *Biochemistry 36*:6009–6016.

Hol WGJ, van Duijnen PT, Berendsen HJC. 1978. The $\alpha$-helix dipole and the properties of proteins. *Nature 273*:443–446.

Horovitz A, Serrano L, Avron B, Bycroft M, Fersht AR. 1990. Strength and cooperativity of contributions of surface salt bridges to protein stability. *J Mol Biol 216*:1031–1044.

Hurley JH, Baase WA, Matthews BW. 1992. Design and structural analysis of alternative hydrophobic core packing arrangements in bacteriophage T4 lysozyme. *J Mol Biol 224*:1143–1159.

Imada K, Sato M, Tanaka N, Katsube Y, Matsuura Y, Oshima T. 1991. Three-dimensional structure of a highly thermostable enzyme, 3-isopropylmalate dehydrogenase of *Thermus thermophilus* at 2.2 Å resolution. *J Mol Biol 222*:725–738.

Jaenicke R. 1996. Glyceraldehyde-3-phosphate dehydrogenase from *Thermotoga maritima*: Strategies of protein stabilization. *FEMS Microbiol Rev 18*:215–224.

Jaenicke R, Böhm G. 1998. The stability of proteins in extreme environments. *Curr Opin Struct Biol 8*:738–748.

Kabsch W, Sander C. 1983. Dictionary of protein secondary structure: Pattern of recognition of hydrogen-bonded and geometrical features. *Biopolymers 22*:2577–2637.

Kallwass HKW, Surewicz WK, Parris W, Macfariane ELA, Luyten MA, Kay CM, Gold M, Jones JB. 1992. Singe amino acid substitutions can further increase the stability of a thermophilic L-lactate dehydrogenase. *Protein Eng 5*:769–774.

Kelly CA, Nishiyama M, Ohnishi Y, Beppu T, Birktoft JJ. 1993. Determinants of protein thermostability observed in the 1.9-Å crystal structure of malate dehydrogenase from the thermophilic bacterium *Thermus flavus*. *Biochemistry 32*:3913–3922.

Kirino H, Aoki M, Aoshima M, Hayashi Y, Ohba M, Yamagishi A, Wakagi T, Oshima T. 1994. Hydrophobic interaction at the subunit interface contributes to the thermostability of 3-isopropylmalate dehydrogenase from an extreme thermophile, *Thermus thermophilus*. *Eur J Biochem 220*:275–281.

Korkhin Y, Frolow F, Bogin O, Peretz M, Kalb(Gilboa) AJ, Burstein Y. 1996. Crystalline alcohol dehydrogenases from the mesophilic bacterium *Clostridium beijerinckii* and the thermophilic bacterium *Thermoanaerobium brockii*: Preparation, characterization and molecular symmetry. *Acta Crystallogr D52*:882–886.

Korkhin Y, Kalb(Gilboa) AJ, Peretz M, Bogin O, Burstein Y, Frolow F. 1998. NADP-dependent bacterial alcohol dehydrogenases: Crystal structure, cofactor binding and cofactor specificity of the ADHs of *Clostridium beijerinckii* and *Thermoanaerobacter brockii*. *J Mol Biol 278*:965–979.

Korndorfer I, Steipe B, Huber R, Tomschy A, Jaenicke R. 1995. The crystal structure of holo-glyceraldehyde-3-phosphate dehydrogenase from the hyperthermophilic bacterium *Thermotoga maritima* at 2.5 Å resolution. *J Mol Biol 246*:511–521.

Kraulis P. 1991. MOLSCRIPT: A program to produce both detailed and schematic plots of protein structures. *J Appl Crystallogr 24*:946–950.

Lamed RJ, Zeikus JG. 1981. Novel NADP-linked alcohol-aldehyde/ketone oxidoreductase in thermophilic ethanologenic bacteria. *Biochem J 195*:183–190.

MacBeath G, Kast P, Hilvert D. 1998. Redesigning enzyme topology by directed evolution. *Science 279*:1958–1961.

Matthews BW, Nicholson H, Becktel WJ. 1987. Enhanced protein thermostability from site-directed mutations that decrease the entropy of unfolding. *Proc Natl Acad Sci USA 84*:6663–6667.

Matthews BW, Weaver LH, Kester WR. 1974. The conformation of thermolysin. *J Biol Chem 249*:8030–8044.

Merritt EA, Murphy ME. 1994. RASTER 3D version 2.0. A program for photorealistic molecular graphics. *Acta Crystallogr D50*:869–873.

Moriyama H, Onodera K, Sakurai M, Tanaka N, Kirino KH, Oshima T, Katsube Y. 1995. The crystal structures of mutated 3-isopropylmalate dehydrogenase from *Thermus thermophilus* HB8 and their relationship to the thermostability of the enzyme. *J Biochem (Tokyo) 117*:408–413.

Nicholls A, Sharp K, Honig B. 1991. Protein folding and association—Insights from the interfacial and thermodynamic properties of hydrocarbons. *Proteins 11*:281–296.

Nicholson H, Becktel WJ, Matthews BW. 1988. Enhanced protein thermostability from designed mutations that interact with alpha-helix dipoles. *Nature 336*:651–656.

Peretz M, Bogin O, Tel-Or S, Cohen A, Li G, Chen J-S, Burstein Y. 1997. Molecular cloning, nucleotide sequencing, and expression of genes encoding alcohol dehydrogenases from the thermophile *Thermoanaerobacter brockii* and the mesophile *Clostridium beijerinckii*. *Anaerobe 3*:259–270.

Peretz M, Burstein Y. 1989. Amino acid sequence of alcohol dehydrogenase from the thermophilic bacterium *Thermoanaerobium brockii*. *Biochemistry 28*:6549–6555.

Perutz MF. 1978. Electrostatic effects in proteins. *Science 201*:1187–1191.

Perutz MF, Raidt H. 1975. Stereochemical basis of heat stability in bacterial ferredoxins and in haemoglobin A2. *Nature 255*:256–259.

Russell RJ, Hough DW, Danson MJ, Taylor GL. 1994. The crystal structure of citrate synthase from the thermophilic archaeon *Thermoplasma acidophilum*. *Structure 2*:1157–1167.

Salminen T, Teplyakov A, Kankare J, Cooperman BS, Lahti RAG. 1996. An unusual route to thermostability disclosed by the comparison of *Thermus thermophilus* and *Escherichia coli* inorganic pyrophosphatases. *Protein Sci 5*:1014–1025.

Sterner R, Vogl T, Hinz HJ, Penz F, Hoff R, Foll R, Decker H. 1995. Extreme thermostability of tarantula hemocyanin. *FEBS Lett 364*:9–12.

Tanner JJ, Hecht RM, Krause KL. 1996. Determinants of enzyme thermostability observed in the molecular structure of *Thermus aquaticus* D-glyceraldehyde-3-phosphate dehydrogenase at 2.5 angstrom resolution. *Biochemistry 35*:2597–2609.

Tomschy A, Böhm G, Jaenicke R. 1994. The effect of ion pairs on the thermal stability of D-glyceraldehyde 3-phosphate dehydrogenase from the hyperthermophilic bacterium *Thermotoga maritima*. *Protein Eng 7*:1471–1478.

Van den Burg B, Vriend G, Veltman OR, Venema G, Eijsink VG. 1998. Engineering an enzyme to resist boiling. *Proc Natl Acad Sci USA 95*:2056–2060.

Vetriani C, Maeder DL, Tolliday N, Yip KSP, Stillman TJ, Britton KL, Rice DW, Klump HH, Robb FT. 1998. Protein thermostability above 100 °C: A key role for ionic interactions. *Proc Natl Acad Sci USA 95*:12300–12305.

Villeret V, Clantin B, Tricot C, Legrain C, Roovers M, Stalon V, Glansdorff N, Van Beeumen J. 1998. The crystal structure of *Pyrococcus furiosus* ornithine carbamoyltransferase reveals a key role for oligomerization in enzyme stability at extremely high temperatures. *Proc Natl Acad Sci USA 95*:2801–2806.

Vriend G. 1990. WHATIF: A molecular modeling and drug design program. *J Mol Graph 8*:52–56.

Walker JE, Wonacott AJ, Harris JI. 1980. Heat stability of a tetrameric enzyme, D-glyceraldehyde-3-phosphate dehydrogenase. *Eur J Biochem 108*:581–586.

Wallon G, Kryger G, Lovett ST, Oshima T, Ringe D, Petsko GA. 1997. Crystal structures of *Escherichia coli and Salmonella typhimurium* 3-isopropylmalate dehydrogenase and comparison with their thermophilic counterpart from *Thermus thermophilus*. *J Mol Biol 266*:1016–1031.

Watanabe K, Chishiro K, Kitamura K, Suzuki Y. 1991. Proline residues responsible for thermostability occur with high frequency in the loop regions of an extremely thermostable oligo-1,6-glucosidase from *Bacillus thermoglucosidasius* KP1006. *J Biol Chem 266*:24287–24294.

Watanabe K, Masuda T, Ohashi H, Mihara H, Suzuki Y. 1994. Multiple proline substitutions cumulatively thermostabilize *Bacillus cereus* ATCC7064 oligo-1,6-glucosidase. Irrefragable proof supporting the proline rule. *Eur J Biochem 226*:277–283.

Yip KSP, Stillman TJ, Britton KL, Artymiuk PJ, Baker PJ, Sedelnikova SE, Engel PC, Pasquo A, Chiaraluce R, Consalvi V, Scandurra R, Rice DW. 1995. The structure of *Pyrococcus furiosus* glutamate dehydrogenase reveals a key role for ion-pair networks in maintaining enzyme stability at extreme temperatures. *Structure 3*:1147–1158.

Zeikus JG, Hegge PW, Anderson MA. 1979. *Thermoanaerobium brockii* gen. nov. and sp. nov., A new chemoorganotrophic, caldoactive, anaerobic bacterium. *Arch Microbiol 122*:41–48.